

# Sliding friction of polyethylene on ice: tribometer measurements

L. Bäurle<sup>a,b</sup>, D. Szabó<sup>a</sup>, M. Fauve<sup>a</sup>, H. Rhyner<sup>a</sup> and N.D. Spencer<sup>b,\*</sup>

<sup>a</sup>WSL, Swiss Federal Institute for Snow and Avalanche Research SLF, CH-7260 Davos, Switzerland

<sup>b</sup>Department of Materials, ETH Zurich, CH-8093 Zurich, Switzerland

Received 22 June 2006; accepted 28 August 2006; published online 18 October 2006

It is well known that the low kinetic friction experienced when sliding on snow and ice is due to water films generated through frictional heating. There is, however, uncertainty concerning the thickness and the distribution of these water films. Since direct observation of the water films is difficult, tribometer studies coupled with temperature measurements have been carried out on a large-scale, pin-on-disc tribometer (diameter 1.80 m). IR sensors were used to measure the temperature of the ice track in front of and behind the contact region. In addition, thermocouples integrated into the polyethylene slider measured the temperature close to the interface. The kinetic friction between polyethylene and ice has been measured as a function of temperature, velocity, load, and apparent contact area. The friction coefficient, as well as the temperature increase of the slider and the ice track, depends on all of these parameters. Interpretation of the results is given on the basis of hydrodynamic lubrication, taking into account the generation and shearing of thin water films in the contact regions.

**KEY WORDS:** ice friction, hydrodynamic lubrication, friction test methods, heat transfer

## 1. Introduction

It was long believed, erroneously, that the low kinetic friction experienced while skiing is due to pressure melting, i.e. that snow or ice melts under pressure to produce a film of water, which lubricates the system [1]. Strong evidence later suggested that the low friction is due to a partial water layer formed by frictional heating [2]. A highly conductive slider displays higher friction than one that is well insulated, indicating that heat conduction plays a major role in ice friction. Quantitative models for the frictional heating theory were developed [3,4] and verified experimentally [5]. Frictional heat is conducted into both slider and ice, thereby raising the ice surface to its melting point. The heat consumed by melting is small, most of it being conducted away. The frictional force then arises due to viscous shear of the water layers between slider and ice. The real contact area between a slider and snow has been determined by observing the snow surface through a microscope after a sliding experiment and found to be around 4% [6]. The average diameter of contacts flattened by frictional melting was found to be around 200  $\mu\text{m}$ . The thickness of the water films formed upon sliding on snow has been measured by a capacitive probe built into a ski, and proposed to amount to 5–14  $\mu\text{m}$  [7]. A more recent study applied fluorescence spectroscopy, combined with a pin-on-rotating-ice-disc experiment, to detect the formation of water films. At

velocities below 0.1  $\text{m s}^{-1}$ , water films, if present, must be below 100 nm in thickness, and thus much thinner than predicted before [8]. In field and laboratory measurements, friction was found to be lowest at around  $-3\text{ }^\circ\text{C}$  and to increase at low temperatures, as well as for temperatures close to  $0\text{ }^\circ\text{C}$  [9].

Classical friction laws for plastically deforming materials do not hold for ice. As will be seen, friction can be very much dependent on load, velocity, and apparent contact area.

Discussion of our results is based upon the assumption that initial contact of the slider with ice leads to (dry) frictional heating, liberating melt-water, which subsequently lubricates further passage of the slider. The initial frictional heat generation rate,  $P$ , can be expressed as

$$P = \mu \cdot F_n \cdot v = F_f \cdot v, \quad (1)$$

where  $F_n$  is the load,  $F_f$  is the friction force, and  $v$  is the velocity. Alternatively, the total heat flux  $q'' = P/A$  through the area  $A$  into the slider and the ice can be written as

$$q'' = v \cdot \sigma_k, \quad (2)$$

where  $\sigma_k$  is the shear stress necessary to slide two surfaces with relative velocity  $v$ . For an estimate, the shear stress is written as  $\sigma_k = \mu \sigma_0$ , where the perpendicular stress  $\sigma_0$  in a contact spot is assumed to be equal to the penetration hardness of the ice. If all heat were conducted into the ice (figure 1), the temperature increase at the interface would amount to (see [10], pp. 251–254)

\*To whom correspondence should be addressed.  
E-mail: nicholas.spencer@mat.ethz.ch

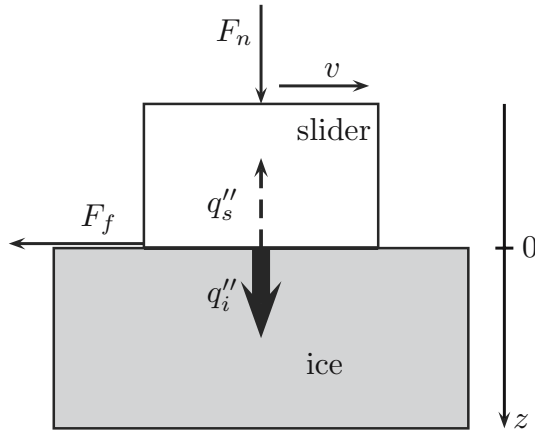


Figure 1. A solid sliding against ice along a planar surface separated by a thin lubricating layer of water. Assume that the heat flux  $q''$  flows primarily into the lower solid.

$$\Delta T = 2 \cdot q'' \cdot \left( \frac{t}{\pi \cdot \lambda \cdot c_p \cdot \rho} \right)^{\frac{1}{2}}, \quad (3)$$

where  $\lambda$ ,  $c_p$ , and  $\rho$  are the thermal conductivity, the specific heat capacity, and the density of the material, respectively. For the diameter of a contact spot,  $D = 200 \mu\text{m}$  is assumed [6]. Using  $v = 1 \text{ m s}^{-1}$  results in a time of contact of approximately  $2 \times 10^{-4} \text{ s}$  and, according to equation (3), to a temperature increase at the interface of 40 K for  $\mu = 0.3$  (dry friction). The exact thickness of the water films is not easy to calculate, however, since when a water film starts to form, the sliding friction drops rapidly, resulting in a concomitant drop in the frictional heat generation. Using the expression for hydrodynamic lubrication

$$\mu = \frac{\eta \cdot v}{h_{\text{wf}} \cdot \sigma_0} \quad (4)$$

where  $\eta$  is the kinematic viscosity of water at 0 °C, even a  $h_{\text{wf}} = 10 \text{ nm}$  thick water layer between two (smooth) surfaces would result in a friction coefficient of about 0.01 (penetration hardness of ice:  $\sigma_0 \approx 2 \times 10^7 \text{ Nm}^{-2}$ ,  $v = 1 \text{ m s}^{-1}$ ). It is assumed that the pressure at the contacts does not reach such high values (due to creep), and therefore thicker water layers are required for low friction. Alternatively, using  $\sigma_0 = F_n/A_{\text{real}}$  and  $\Delta_{\text{rel}} = A_{\text{real}}/A_{\text{app}}$ , the relative real contact area, equation (4) can be rewritten to yield the friction force:

$$F_f = \frac{\eta \cdot v \cdot A_{\text{real}}}{h_{\text{wf}}} = \eta \cdot v \cdot A_{\text{app}} \cdot \frac{\Delta_{\text{rel}}}{h_{\text{wf}}}. \quad (5)$$

How  $h_{\text{wf}}$  and  $\Delta_{\text{rel}}$  are linked depends on the roughness of the sliding partners. For simplicity, it is assumed that a perfectly flat slider slides on “rough” ice (roughness on the order of  $R_a = 0.1\text{--}1 \mu\text{m}$ , Gaussian-like height distribution). We assume that the slider “slices off” ice asperities by melting, the amount depending on the water-film thickness. Figure 2 illustrates this mecha-

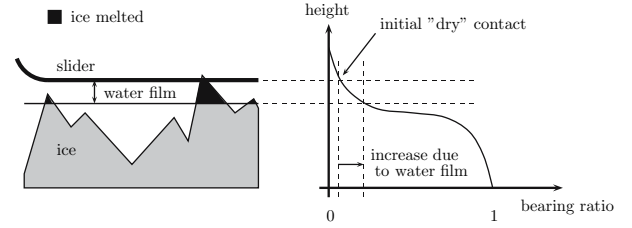


Figure 2. Relation between the water-film thickness and the real contact area (bearing ratio). Melting of ice corresponds to a slicing off, and leads to the growth of existing contacts, and the formation of new contacts.

nism, and shows the relation between water-film thickness and relative real contact area (i.e. bearing ratio). There are two competing processes: thicker water films lead to lower friction (predominantly at lower temperatures), while more water leads to higher real contact area, and therefore higher friction. In brief, the sliding process is an interplay of frictional heat conducted away and available for the melting of ice, water-film thickness, and real contact area.

A number of investigators have set up experiments in order to measure friction of different materials on ice [2,9,11,12,13]. It was recognized that the warming of the ice track presents a problem, and thus either small tribometers (different designs: pin-on-disc, rotating drum, linear devices) with low sliding velocities ( $v < 1 \text{ m s}^{-1}$ ) were used, or larger-scale devices were built. Most of the latter encountered problems with vibrations, reducing the accuracy of the measurement. Although it was recognized that the low kinetic friction is due to the melting of the ice surface, and thus is strongly influenced by temperature, none of the earlier experiments had adequate temperature control. Tribological measurements on snow present enormous reproducibility challenges and therefore, in this study, the polyethylene-ice interface has been investigated as a first approximation. In fact, this is also of relevance to skiing under racing conditions, where the piste consists of compact, icy snow. Friction experiments of polyethylene on ice with monitored temperature evolution at or near the interface have been carried out to determine how much heat is generated in the friction process.

## 2. Experimental

### 2.1. Tribometer

A 1.80 m-diameter tribometer has been designed, built and placed in a cold chamber with an accessible temperature range of  $T_{\text{air}} = -20 \text{ °C}$  to  $+1 \text{ °C}$ . Velocity can be varied between  $v = 0.5 \text{ m s}^{-1}$  and  $20 \text{ m s}^{-1}$ , and load between roughly  $F_n = 20 \text{ N}$  and  $100 \text{ N}$ . The length of the sample in the direction parallel to the sliding direction is  $l = 4 \text{ cm}$ . The width of the apparent contact region can be adjusted between  $w = 0.5\text{--}2.5 \text{ cm}$  by

setting the width of an elevated track carved into the ice. An apparent contact area of  $A_{\text{app}} = 2 \text{ cm}^2$  to  $10 \text{ cm}^2$  results. The apparatus consists of the rotating table carrying the ice annulus, and two arms for holding the slider and the ice-surface-preparation tools (figure 3). Figure 4 shows the assembly of the friction-force-measurement unit: A strain-gauge load cell (Interface MB-10, Scottsdale, AZ, USA) measures the shear force between the upper (fixed) and the lower (movable) aluminum plate, the latter holding the slider. The normal force is transmitted via two vertical brass plates. A spring acts as overload protection. The samples consist of a block of polyethylene ( $40 \text{ mm} \times 40 \text{ mm} \times 9 \text{ mm}$ ), attached to a 10 mm thick foam rubber pad (polyurethane elastomer, glass temperature  $T_g \sim -40 \text{ }^\circ\text{C}$ ), which is then attached to the aluminum plate by double-faced adhesive tape. The foam rubber is necessary to ensure a parallel contact, and to compensate for unevenness of the track and vibrations. The signal from the load cell is amplified, read into a PC via a PCI-6034E card, and processed in Labview (National Instruments, Austin, TX, USA). The compressor and the fans of the chamber-cooling system induce vibrations, and thus the device must be decoupled from the structure of the cold chamber. It is therefore directly attached to the concrete foundation beneath the chamber. Even a very stiff construction can, at high rotational velocities, induce considerable vibrations if not well balanced. The tribometer was therefore balanced in situ using a Vibrotest 60 device (Brüel & Kjaer, Naerum, Denmark).

For the ice preparation, a 2–5 cm thick ice annulus is frozen onto the table, layer by layer. The thickness should not surpass some millimeters per layer, otherwise crack formation and air inclusions become severe. To account for the expansion of the ice, 2 cm thick foam rubber is used as a side wall on the outer side of the track. For the last couple of layers, or to refresh an existing ice surface, only thin layers of water are frozen on by means of a wet towel. Freezing of ice in this way still leads to a relatively uneven

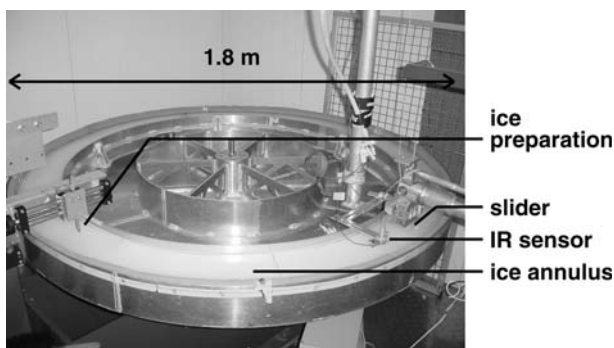


Figure 3. Tribometer. It consists of the rotating table carrying the ice annulus, and two arms for holding the ice-surface-preparation tools (left) and the friction-force-measurement unit, to which the slider is attached (right). IR temperature sensors measure the ice temperature in front of and behind the slider.

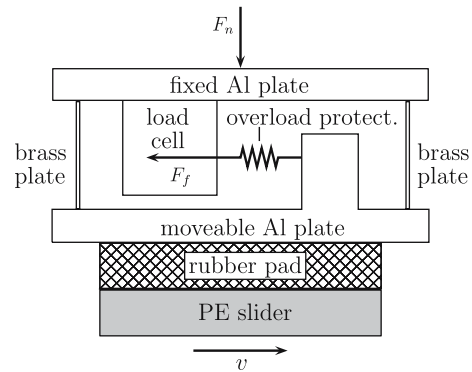


Figure 4. Design of the friction-force measurement. The PE slider is attached to the lower aluminum plate. A strain-gauge load cell measures the shear force between upper and lower aluminum plate.

surface. The surface is therefore shaved down to a constant height using the principle of a lathe, by means of a steel bar of width 2 mm at the tip, which can be moved manually in vertical and radial directions by linear-motion stages. For most of the experiments, an elevated track is carved out of the ice, to prevent the slider edge from cutting into the annulus.

Measurements are conducted according to the following procedure: 1. Preparation of the ice surface and setting of the track width ( $w$ ). 2. Run-in period: the slider to be measured is slid for about 5 min at high load ( $F_n = 84 \text{ N}$ ) and velocity ( $v = 5\text{--}10 \text{ m s}^{-1}$ ). 3. Slider and ice are left to cool for 5 min. 4. Tribometer is set to the desired velocity, recording of the data is started, and the slider is lowered onto the running tribometer. 5. After 3–5 min, recording is stopped, slider lifted, and the procedure is repeated from step 3. Along with the tribological measurements, repeated visual checking of the ice surface and detection of possible vibration is carried out. A new ice surface is prepared if necessary.

## 2.2. Temperature measurements

A number of techniques can be used to measure transient interface temperature rise at sliding interfaces, e.g. thermocouples, thermistors, radiation-detection techniques (for a complete summary, see [14], pp. 314–326). For a first estimate of the heat generated in the frictional process, a Varioscan 3021-ST infrared camera (Jenoptik, Jena, Germany; image format:  $360 \times 240$  pixels, frame rate: 1 Hz) was used to take images of the track behind the slider (figure 5). A significant increase of the temperature can be observed. However, the obtained values cannot be interpreted quantitatively, since the resolution of the camera is too low to resolve single contact spots and they thus represent an average of the temperatures encountered at the surface; i.e. spots that have been in contact with the slider (real contact area),

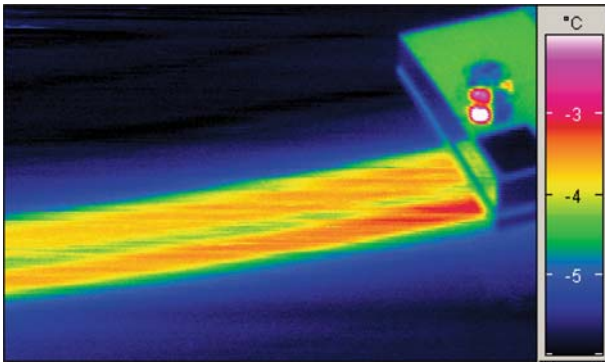


Figure 5. Heating of the track behind the slider. Infrared image. Temperature of the surrounding ice is  $-6\text{ }^{\circ}\text{C}$ , maximum temperature measured is  $-3\text{ }^{\circ}\text{C}$   $F_n = 84\text{ N}$ ,  $A_{\text{app}} = 10\text{ cm}^2$ ,  $v = 5\text{ m s}^{-1}$ .

and where melting took place, as well as regions that have not experienced a major temperature increase. Moreover, the radiation measured by the camera is emitted not only from the very surface of the ice, but also from regions slightly below the surface. This effect, too, makes it hard to obtain quantitative temperature values using IR measurements. Furthermore, the temperature distribution in the track suggests that the slider does not evenly contact the ice.

IR sensors (Omega OS36-K-50F, Stamford, CT, USA) are used to measure the temperature of the track in front of and behind the slider. The IR sensor signals, as well as the standard thermocouple voltages, are read in via a USB TC08 data recorder (Pico Technology, Cambridgeshire, UK) and processed in Labview.

Since temperature measurement at the very interface is not easily accomplished, temperature is measured just above the interface within the slider. Holes of diameter  $1.5\text{ mm}$  are drilled into the slider from the top to within  $0.2 \pm 0.1\text{ mm}$  of the lower surface. Thin thermocouples (Omega CHAL-002, wire diameter of  $50\text{ }\mu\text{m}$ ) are glued into the holes using a two-component resin (Araldite AW 136H and Aradur 5049-1, Huntsman, Belgium). Heat conductivity and capacity of polyethylene and the resin differ only slightly and should therefore not affect the heat conduction into the slider. The thermocouples are located on the central axis of the slider (along the sliding direction) after (from front to back)  $1\text{ cm}$  (denoted TC1),  $2\text{ cm}$  (TC2), and  $3\text{ cm}$  (TC3). Monitoring of the location of the thermocouples as well as detection of possible air inclusions are conducted using an X-ray computer tomograph. From X-ray scans, it is possible to determine the position of the thermocouple to  $\pm 50\text{ }\mu\text{m}$ . 3D scans show negligible air inclusions. The slider with the built-in thermocouples is calibrated in an ice-water mixture.

### 3. Results and discussion

Figure 6 shows the recorded signals of a typical tribological measurement. The slow increase of the friction

force is attributed to an increase in real contact area due to polishing of the ice track. In order to obtain a single friction coefficient value, this increase is fitted by an exponential function (dashed line) approaching a constant value, and the latter is taken as the steady-state friction coefficient. The temperatures recorded by the thermocouples (circles) in the slider show a delayed increase but also reach a steady state after about 2 min. The temperatures recorded by the IR sensors in front of and behind the slider (triangles) can only be interpreted qualitatively; they show an average ice surface temperature of former contact spots (having been at  $0\text{ }^{\circ}\text{C}$ ) and regions that have not made contact (having remained below  $0\text{ }^{\circ}\text{C}$ ).

#### 3.1. Temperature dependence

Water-film thickness is expected to increase with temperature, due to lower temperature gradients and correspondingly less heat lost to conduction. Figure 7 shows the temperature dependence of friction. At low temperatures (below  $-2\text{ }^{\circ}\text{C}$ ), increased temperature leads to decreased friction. Above  $-2\text{ }^{\circ}\text{C}$ , however, increased temperature leads to higher friction. This can be explained by increased melt water leading to higher real contact areas.

The subsequent discussion of the measurement is divided into three different temperature regimes, which show different dependencies of the friction force on the parameters velocity and load.

#### 3.2. Low temperatures: $T_{\text{air}} \leq -10\text{ }^{\circ}\text{C}$

At temperatures of  $T_{\text{air}} = -10\text{ }^{\circ}\text{C}$  and below, a major part of the frictional heat generated is expected to be conducted into slider and (mainly) ice. Only little heat is therefore available for melting ice, and only thin water films result. The decreasing friction with increasing velocity (figure 8) can be explained by more heat being available to melt ice, and more water increasing the average water-film thickness (while real contact area negligibly increases), which leads to better lubrication and lower friction. Earlier calculations and measurements showed the friction coefficient to follow  $v^{-0.5}$  [3,4]. Friction force is observed to increase linearly with load (figure 9). Note the increased friction for the larger apparent contact area. The temperature increase in the slider, however, does not depend on the contact area. This dependence of friction on contact area is, at first sight, not in accordance with classical friction theories. A peculiarity in ice friction is, however, that the friction process generates its own lubricant. Assuming that the initial dry friction process follows classical friction laws, the energy that is released per area is higher for a lower contact area. Therefore, the transition from dry to lubricated friction happens at an earlier position along

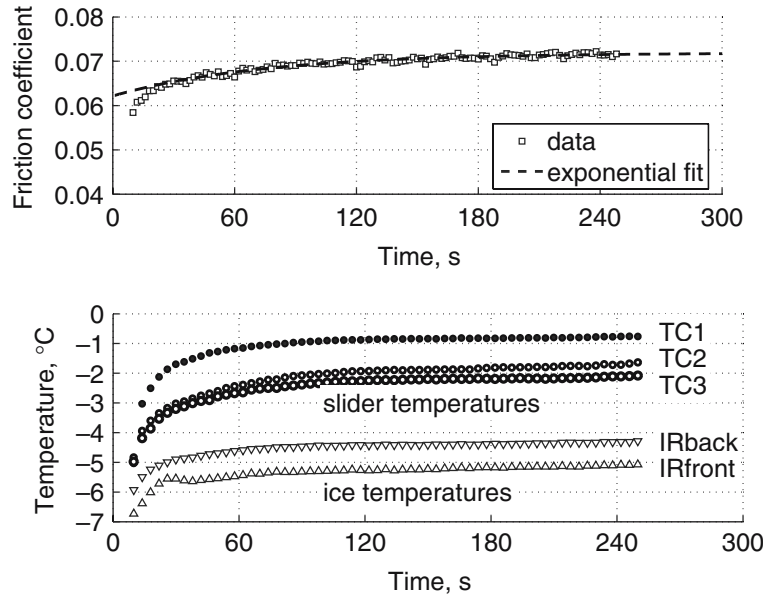


Figure 6. Typical friction measurement showing friction coefficient (above) and temperature evolution (below) measured.  $T_{\text{air}} = -5\text{ }^{\circ}\text{C}$ ,  $F_n = 84\text{ N}$ ,  $v = 5\text{ m s}^{-1}$ , and  $A_{\text{app}} = 4\text{ cm}^2$ .

the sample for the smaller contact area; a larger portion of a contact is lubricated hydrodynamically and thus the whole system exhibits lower friction. The corresponding increase in temperature is expected to be small and presumably lies within the errors of the measurement.

3.3. Intermediate temperatures:  $-10^{\circ}\text{ C} < T_{\text{air}} \leq -1^{\circ}\text{ C}$

At intermediate temperatures around  $T_{\text{air}} = -5\text{ }^{\circ}\text{C}$ , friction is low and does not depend on velocity in the range observed (figure 10). The measured temperatures in the slider are very much dependent on velocity, however. Temperature increases proportionally to heat generation rate (equation 1) up to  $v = 3\text{ m s}^{-1}$ .

Assuming that all frictional heat is conducted into the slider, a calculation for the slope of the temperature rise vs. velocity curve (equations 1 and 3) results in a value that is 150 times higher than the experimentally obtained  $1.6\text{ K m}^{-1}\text{ s}$ . This confirms that only a small fraction of the frictional heat enters the slider ( $\lambda_{\text{PE}} = 0.34\text{ W m}^{-1}\text{ K}^{-1}$ ); most if it is conducted into the ice ( $\lambda_{\text{ice}} = 2.2\text{ W m}^{-1}\text{ K}^{-1}$ ), or used in the phase change from ice to water. Temperature in the slider at a depth of  $0.2\text{ mm}$  reaches approximately  $T = 0.5\text{ }^{\circ}\text{C}$  for  $v \geq 5\text{ m s}^{-1}$ . The phase transition at  $0^{\circ}$  constitutes an upper temperature limit, the temperature increase flattening off at higher velocities. Heat is consumed in melting ice, and the expected lower friction due to thicker films is balanced by increased real contact area

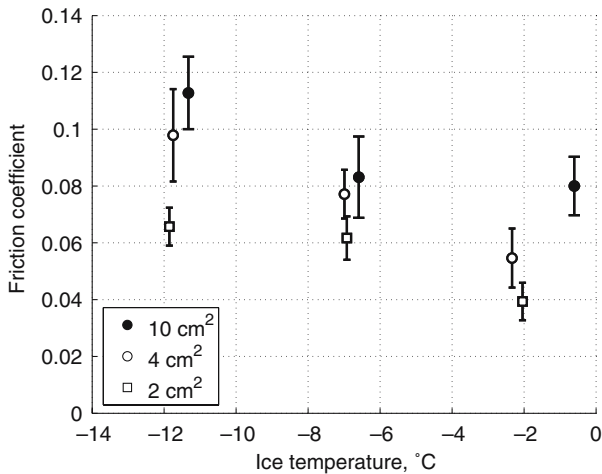


Figure 7. Friction coefficient vs. temperature in a velocity range of  $v = 3\text{--}5\text{ m s}^{-1}$  and a load range of  $F_n = 52\text{ N}$  to  $84\text{ N}$ , summarized and plotted for three different apparent contact areas.

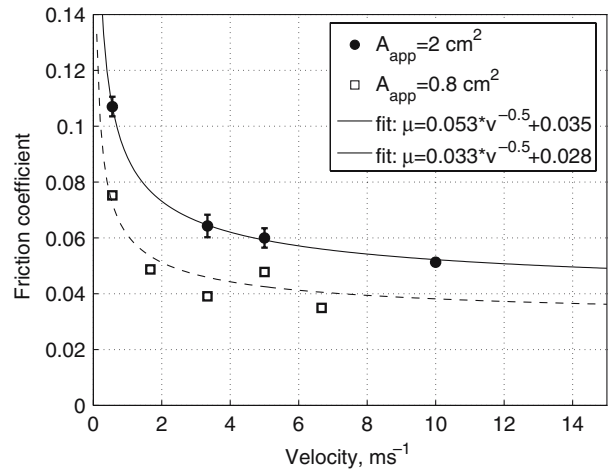


Figure 8. Dependence of friction coefficient on velocity at  $T_{\text{air}} = -10\text{ }^{\circ}\text{C}$  and  $F_n = 84\text{ N}$  for two different apparent contact areas.  $v^{-0.5}$  fit according to [3,4].

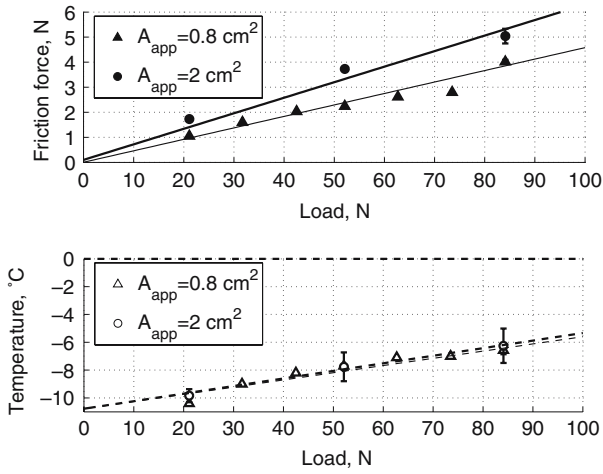


Figure 9. Dependence of friction force and temperature in the slider (TC2) on load at  $T_{\text{air}} = -10\text{ }^\circ\text{C}$ ,  $v = 5\text{ m s}^{-1}$  and contact areas  $A_{\text{app}} = 0.8\text{ cm}^2$  and  $2\text{ cm}^2$ .

and the shear force being proportional to velocity. Assuming a steady state, and thus a linear temperature distribution in the slider (room temperature at the upper side of the slider), the average temperature at the interface can be calculated as  $T \approx -0.4\text{ }^\circ\text{C}$  for velocities  $v \geq 5\text{ m s}^{-1}$  (uncertainty of the thermocouple temperature measurement is  $\pm 0.2\text{ }^\circ\text{C}$ ). Since this temperature is an average of the area in contact at  $T = 0\text{ }^\circ\text{C}$  and the non-contacting region at temperatures below  $T = 0\text{ }^\circ\text{C}$ , it implies that a large fraction of the apparent contact area is at the melting point temperature, and therefore in real contact.

Figure 11 shows the dependence of the friction force on the mean pressure in the apparent contact area considered. The extrapolated friction force at zero pressure (or load) can be used to calculate the relative real contact area according to equation 5. Assuming a film thickness of  $h_{\text{wf}} = 100\text{ nm}$  [8], a relative real contact area of  $\Delta_{\text{rel}} = 0.06$  (6%) results ( $v = 5\text{ m s}^{-1}$ ,

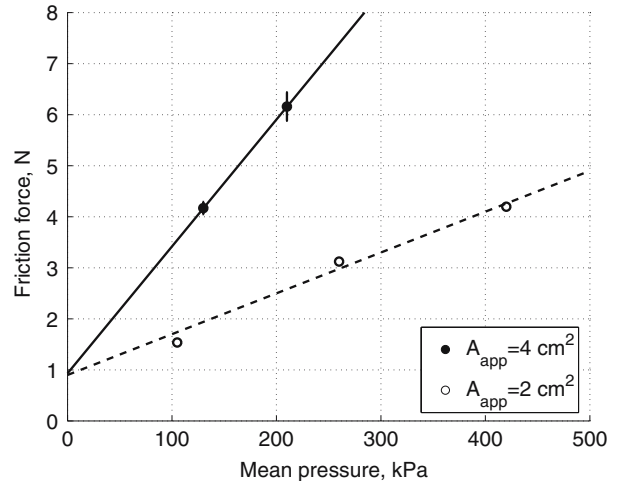


Figure 11. Dependence of friction force on mean pressure at  $T_{\text{air}} = -5\text{ }^\circ\text{C}$  and  $v = 5\text{ m s}^{-1}$  for  $A_{\text{app}} = 2\text{ cm}^2$  and  $4\text{ cm}^2$ .

$A_{\text{app}} = 2\text{ cm}^2$ ,  $F_f = 1\text{ N}$ ). This corresponds to the portion of the slider that is contacting the ice through a water film when neglecting the influence of a normal force. Slider temperatures (figure 10) suggest a higher real contact area, which would correspond to thicker water films. The accuracy of such rough estimates is limited, however.

As for low temperatures, friction increases with increasing  $A_{\text{app}}$  (figure 12). This effect levels off for higher contact areas. We assume that for low contact areas ( $A_{\text{app}} \leq 4\text{ cm}^2$ ), where a higher amount of frictional energy is liberated per unit area, the relative real contact area is close to 100%, and contact spots are located very close to each other. The slope of a fit to the data can be compared to equation 5 to find the quotient of relative real contact area and water-film thickness. A value of  $h_{\text{wf}}/\Delta_{\text{rel}} \approx 0.5\text{ }\mu\text{m}$  is found. For higher contact

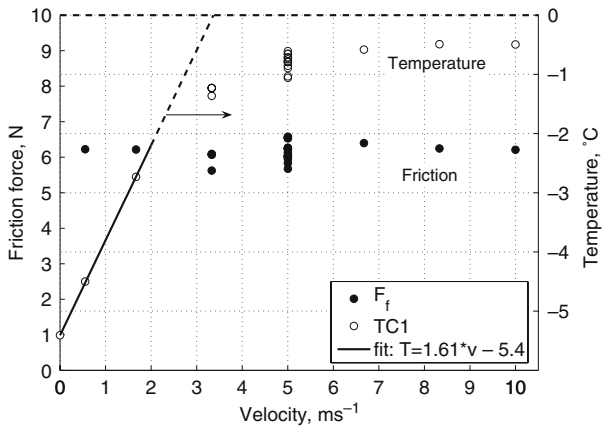


Figure 10. Dependence of friction force and slider temperature close to the interface (after 5 min of measurement) on velocity at  $T_{\text{air}} = -5\text{ }^\circ\text{C}$ ,  $F_n = 84\text{ N}$ ,  $A_{\text{app}} = 4\text{ cm}^2$ .

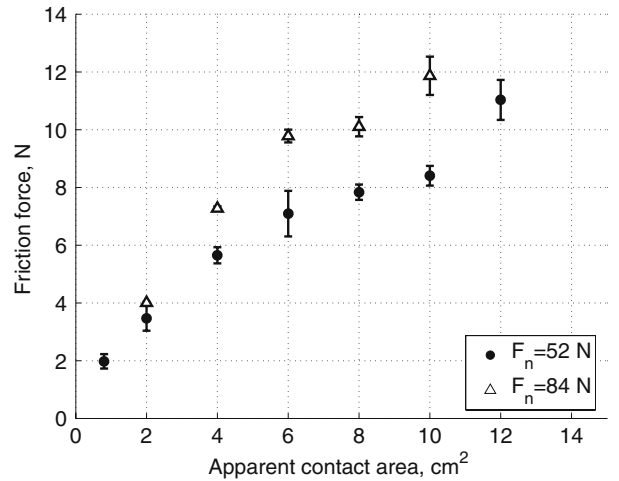


Figure 12. Dependence of friction coefficient on apparent contact area for different loads at  $T_{\text{air}} = -5\text{ }^\circ\text{C}$ . Velocities of  $v = 3.3\text{--}5\text{ m s}^{-1}$  are combined since there is hardly any velocity dependence of the friction coefficient.

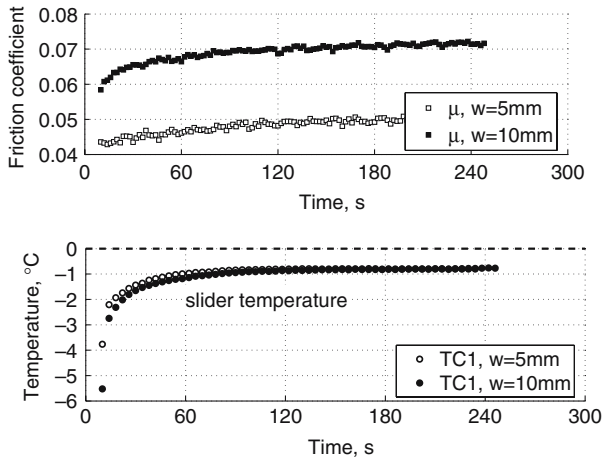


Figure 13. Friction coefficient and slider temperature for  $T_{\text{air}} = -5^\circ\text{C}$ ,  $F_n = 84\text{ N}$ ,  $v = 5\text{ m s}^{-1}$  and track widths of  $w = 5\text{ mm}$  and  $10\text{ mm}$  (slider length:  $40\text{ mm}$ ), corresponding to  $A_{\text{app}} = 2\text{ cm}^2$  and  $4\text{ cm}^2$ .

areas, contact spots start to become more separated from each other and the behavior becomes more classical, i.e. friction starts to be independent of contact area. Temperature evolution in the slider, on the other hand, seems to be slightly dependent on the apparent contact area (figure 13). Note that the friction coefficients measured are similar to values obtained by [9]. The experimental settings (e.g. velocity or sample size) vary considerably in previous studies in the field of ice friction, however, and values are thus difficult to compare.

### 3.4. Temperatures Close to the melting point temperature: $T_{\text{air}} > -1^\circ\text{C}$

At temperatures between roughly  $T_{\text{air}} = -0.5^\circ$  to  $+0.5^\circ$ , heat conduction plays a minor role, and behavior of relatively thick water films can explain the

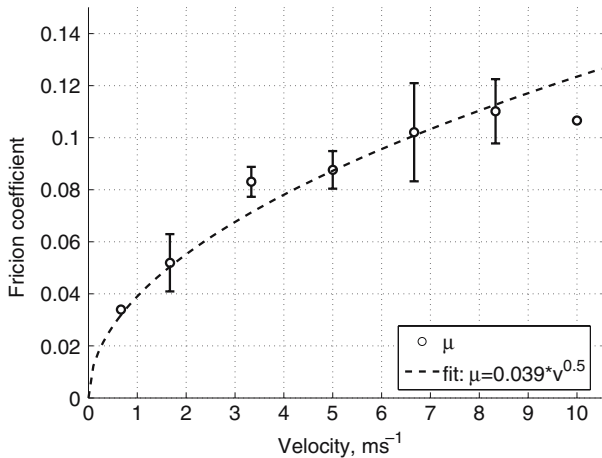


Figure 14. Dependence of friction coefficient on velocity at temperatures close to the melting point (wet conditions) for  $F_n = 52\text{ N}$  and  $A_{\text{app}} = 10\text{ cm}^2$ .

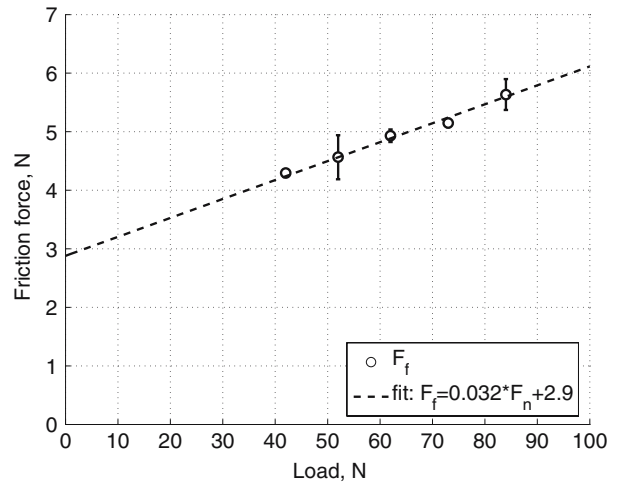


Figure 15. Dependence of friction force on load at temperatures close to the melting point ( $T_{\text{air}} > -1^\circ\text{C}$ ) for  $v = 5\text{ m s}^{-1}$  and  $A_{\text{app}} = 10\text{ cm}^2$ .

dependence of the friction coefficient on velocity and load. Friction is high, due to significantly increased contact area. From [4], water-film thickness is proportional to  $\sqrt{v}$ , thus from equation 5 an overall dependence of  $F_f \sim \sqrt{v}$  results. At zero velocity, the friction coefficient is zero. A linear fit (“valid” in velocity range  $v = 2\text{ m s}^{-1}$  to  $8\text{ m s}^{-1}$ ) to the experimental data in figure 14 yields a slope of 0.0082. Assuming that the relative real contact area is close to 100% at  $0^\circ\text{C}$ , an average water-film thickness of about  $4\text{ }\mu\text{m}$  results (equation 5). This assumption is further confirmed by the fact that the slider reaches temperatures above  $0^\circ\text{C}$  in some measurements. Based on the present understanding, this is only possible if the relative real contact area reaches 100%, otherwise additional heat would be used to melt more water and increase the real contact area.

The extrapolated friction force (see figure 15) at zero load of  $F_f = 2.9\text{ N}$  corresponds well with equation (5) for an assumed relative real contact area close to 100% (continuous water film) and an average water-film thickness of about  $3\text{ }\mu\text{m}$ . Lower contact area would correspond to proportionally thinner films. The friction coefficient decreases for increasing load. This can be explained by more heat released per area leading to thicker water films and, therefore, a lower friction coefficient.

## 4. Conclusion and outlook

By means of a purpose-built tribometer, it has been possible to measure friction of ski-base materials on ice reproducibly, as well as monitor temperature evolution in the slider and in the ice. Temperature and sliding velocity can be chosen according to conditions encountered in real skiing, while load and sample size have to be adjusted to the laboratory scale.

A combined dry friction and hydrodynamic approach is successfully used to explain the friction forces and temperature evolutions measured. The main factors determining friction are the thickness of the water films and the relative real contact area. Both these factors can vary over more than an order of magnitude, depending mostly on temperature and velocity. Estimates suggest that for intermediate temperatures ( $T_{\text{air}} = -10\text{ °C}$  to  $-1\text{ °C}$ ), water-film thickness should be around 100–200 nm, relative real contact area around 10%. Under wet conditions, water-film thickness amounts to some microns and relative real contact area approaches 100%. The friction coefficient decreases with increasing load, especially at higher temperatures ( $T_{\text{air}} > -1\text{ °C}$ ).

The main implication for improved sliding behavior of ski bases under real skiing conditions is that apparent contact area matters. Today's ski-preparation techniques alter structures in the 10–100  $\mu\text{m}$  order of magnitude (mean roughness values). Thickness of the water films, however, is at the most a few microns in warm conditions, and much less for cold conditions. Further work aimed at reducing friction between polyethylene and ice must thus focus on the sub-micron level.

### Acknowledgments

This paper is dedicated to the memory of Dr. Daniel Buhl (17.11.1967–15.02.2004). This work was supported by the Swiss Committee for Technology and Innovation

(CTI) and industrial partners: Stöckli Ski and Mammut Sports Group, Switzerland. We thank Bernhard Zingg and co-workers, SLF Davos, Switzerland, for his contributions in designing and constructing the tribometer.

### References

- [1] O. Reynolds, *Papers on Mechanical and Physical Subjects II* (Cambridge University Press, New York, 1901), p. 737.
- [2] F.P. Bowden and T.P. Hughes, *Proc. R. Soc. Lond. A* 172 (1939) 280.
- [3] D.C.B. Evans, J.F. Nye and K.J. Cheesman, *Proc. R. Soc. Lond. A* 347(1651) (1976) 493.
- [4] P. Oksanen and J. Keinonen, *Wear* 78 (1982) 315.
- [5] M. Akkok, C.M.McC. Ettles and S.J. Calabrese, *Trans. ASME* 109 (1987) 552.
- [6] D. Kuroiwa, *J. Glaciol.* 19(81) (1977) 141.
- [7] W. Ambach and B. Mayr, *Cold Regions Sci. Tech.* 5 (1981) 59.
- [8] H. Strausky, J.R. Krenn, F.R. Leitner and F.R. Aussenegg, *Appl. Phys. B* 66 (1998) 599.
- [9] D. Buhl, M. Fauve and H. Rhyner, *Cold Regions Sci. Tech.* 33 (2001) 133.
- [10] B. Persson, *Sliding Friction: Physical Principles and Applications* (Springer, Berlin, 2000).
- [11] W. Gnoerich and K.A. Grosch, *J. Inst. Rubber Industry* 6 (1972) 192.
- [12] J. Keinonen, *Acta Polytechnica Scand. – Appl. Phys. Ser.* 123 (1978).
- [13] A. Lehtovaara, *Kinetic Friction between Ski and Snow*. PhD thesis, Tampere University of Technology (1989).
- [14] B. Bhushan, *Introduction to Tribology* (John Wiley & Sons, New York, 2002).